ELSEVIER

Coordination Chemistry Reviews
150 (1996) 243–264

COORDINATION CHEMISTRY REVIEWS

Chapter 9
Hints on experimental techniques

Contents

9.1. How to record 1D NMR spectra of paramagnetic molecules

All over the book we have underlined that paramagnetic molecules have short nuclear relaxation times. This has to be faced when recording the spectra, and proper measures should be taken to minimize the consequences of the fast nuclear relaxation. For example, a broader line has smaller height than a sharp line, if the number of nuclei is the same and if the spectral width is the same. This, in practice, is going to affect the signal to noise (S/N) ratio. The decrease in S/N can be partially avoided by a proper choice of the acquisition time (or of t_1^{max} and t_2^{max} in 2D spectra). As discussed in Chapter 7, the information content of an FID decays with T_2 of the signal of interest, and therefore acquisition times much longer than T_2 should not be used, unless sharp and ill-resolved signals are also looked for in the spectrum. The reduction in t_1^{max} does not necessarily decrease the number of sampled data points, as often the large spectral widths needed for paramagnetic compounds require a more frequent data point sampling (shortening of the dwell time). Many modern instruments use oversampling techniques, that allow data points to be always sampled at the highest possible speed, thereby optimizing the S/N for any chosen spectral width.

When the spectral width is of hundreds of parts per million, i.e. more than 10^5 Hz on high field instruments, a very short excitation pulse is needed. Of course, high

PII S0010-8545(96)01248-9

power is needed to reach the r.f. energy corresponding to a 90° pulse in a short time. To best exploit the short relaxation times, it is often convenient to use a full 90° excitation pulse and to recycle fast, because magnetization equilibrium is reached quickly. With suitable power supplies and purpose-built probes, short ^{1}H 90° pulses can be achieved (as short as 3.5 μs at 600 MHz). When very large spectral widths are needed, pulses of less than 90° can always be used.

A large spectral width also requires an adequate ADC. For example, an ADC with a minimum dwell time of 2.5 μs covers a spectral width of 400 kHz. Bruker instruments use one ADC to sample both the real and imaginary part of the FID. Therefore, only 200 kHz (267 ppm at 750 MHz) of maximal spectral width are available for such an ADC. Other instruments use two identical ADCs to sample real and imaginary data points, and therefore the whole spectral width determined by the specific minimal dwell time of the ADC can be used. Lower dynamic range ADCs (e.g. 12 bit instead of 16 bit) usually have shorter dwell time, and larger spectral widths can be achieved. We recall that the dynamic range is the maximal number of powers of two that can be used to digitalize the intensity of a signal. The problem of the dynamic range is not important in the presence of signals all of similar intensities. It becomes important when a weak signal is in the presence of a strong signal. This is because when the receiver gain is reduced to accommodate the strong signal within the dynamic range of the ADC, the weak signal and even the noise may have an intensity smaller than the digital threshold of the ADC itself. This problem may be serious in protein ^{1}H NMR at high field, and in general in the presence of undeuterated solvents. For these reasons more and more efficient signal suppression techniques have been developed (see below). As the latest generation of instruments spreads out, however, it turns out that the loss of weak signals because of dynamic range problems is rather seldom. It can be shown that under non-extreme signal suppression conditions the receiver gain is already high enough that a further increase — that could be made possible by a further reduction of the strongest signals — amplifies the noise to the same extent as the signal. This is even more true when large spectral windows are used.

Associated with large spectral widths there are serious baseline problems. These arise from different sources, some of which are unavoidable because they are connected with the physics of the experiment. An ideal experiment would require: (1) a pulse of infinitely short length; (2) no dead time between the end of the pulse and the start of the acquisition; (3) immediate linear response of the receiver at the start of the acquisition; (4) a filter of perfectly rectangular shape. In practice, any physical receiver requires a finite time to reach linear response conditions after it is turned on. This time is of the order of microseconds and can be as long as some tens of microseconds. Therefore, if the receiver is turned on immediately after the end of the pulse, and if the dwell time is short because of large spectral width (for example, 2.5 μs) the first several data points may have an altered intensity. After Fourier transform, this altered intensity is translated into a baseline distortion. To reduce this problem, a dead time of the order of the time required by the receiver to achieve linearity is introduced before starting the acquisition. This dead time may also be useful to avoid acoustic ringing from the probe, which may be a serious problem at

low Larmor frequencies (typically when observing low γ nuclei, or even protons at low fields). Introducing a dead time is equivalent to losing the first few data points in the FID. In turn, this causes a first order dephasing of the signals, i.e. a dephasing that increases with increasing offset from the carrier. First order phase correction again introduces a baseline distortion. Reconstruction of the first points of the FID by linear prediction techniques is very useful in this respect.

The finite duration of the pulse in a way causes the same kind of problems, because nuclei resonating far from the carrier frequency appreciably start precessing during the pulse itself and therefore are dephased. The quality of the probe (Q-factor, reflected power, etc.) also influences the quality of the baseline. Finally, the analog filters used to decrease the noise by filtering out the high frequency noise coming from outside the spectral window are not rectangular, and introduce a baseline distortion. This last problem is virtually eliminated by the latest generation instruments performing digital filtering. As an extreme limit, there is to consider that when nuclear relaxation is of the order of the dead time, precious information on such nuclei is lost before acquisition. This can be the case in paramagnetic solids, but when this occurs the lines are so broad that we are not in the realm of high resolution NMR any longer.

We are now going to discuss some pulse sequences particularly suitable for ^{1}H NMR of paramagnetic molecules when the signals of protons experiencing hyperfine coupling are present together with an overwhelming number of protons which are virtually diamagnetic. This is the case of paramagnetic metalloproteins and of water solutions of both paramagnetic macromolecules or small molecules displaying a strong solvent signal. These sequences can be classified according to three criteria. The first is based on presaturation of one signal or of the signals within a chosen window. After presaturation the excitation pulse is applied. Presaturation can also be achieved off-resonance without actually offsetting the carrier frequency. The second approach is based on pulse sequences that do not excite the solvent frequency or a narrow window of frequencies. These sequences are most useful when exchangeable protons may be saturated upon saturation of the solvent. The third approach is that of using pulse sequences that take advantage of the different T_1 values in order to suppress signals with long T_1 values. In the absence of chemical exchange phenomena, the choice of the strategy is not philosophical but is simply based on suitability to specific samples, specific spectrometers and, to some extent, on personal taste.

9.1.1. Presaturation sequences

The selective saturation of one signal can be achieved with a soft pulse at a given frequency. Selectivity can be further improved by shaping the pulse, for instance as Gaussian [1], sinc [2] (Fig. 9.1(A)) or Hermitian [3] functions. Very successful are the compositions of three (G3, Fig. 9.1(B)) or four (G4) Gaussians (Gaussian cascades) in a single pulse [4]. Shaped pulses are routinely achieved by constructing the desired shape with a relatively large number of short rectangular pulses of variable intensity and phases. A suitable modification of the DANTE [5] sequence

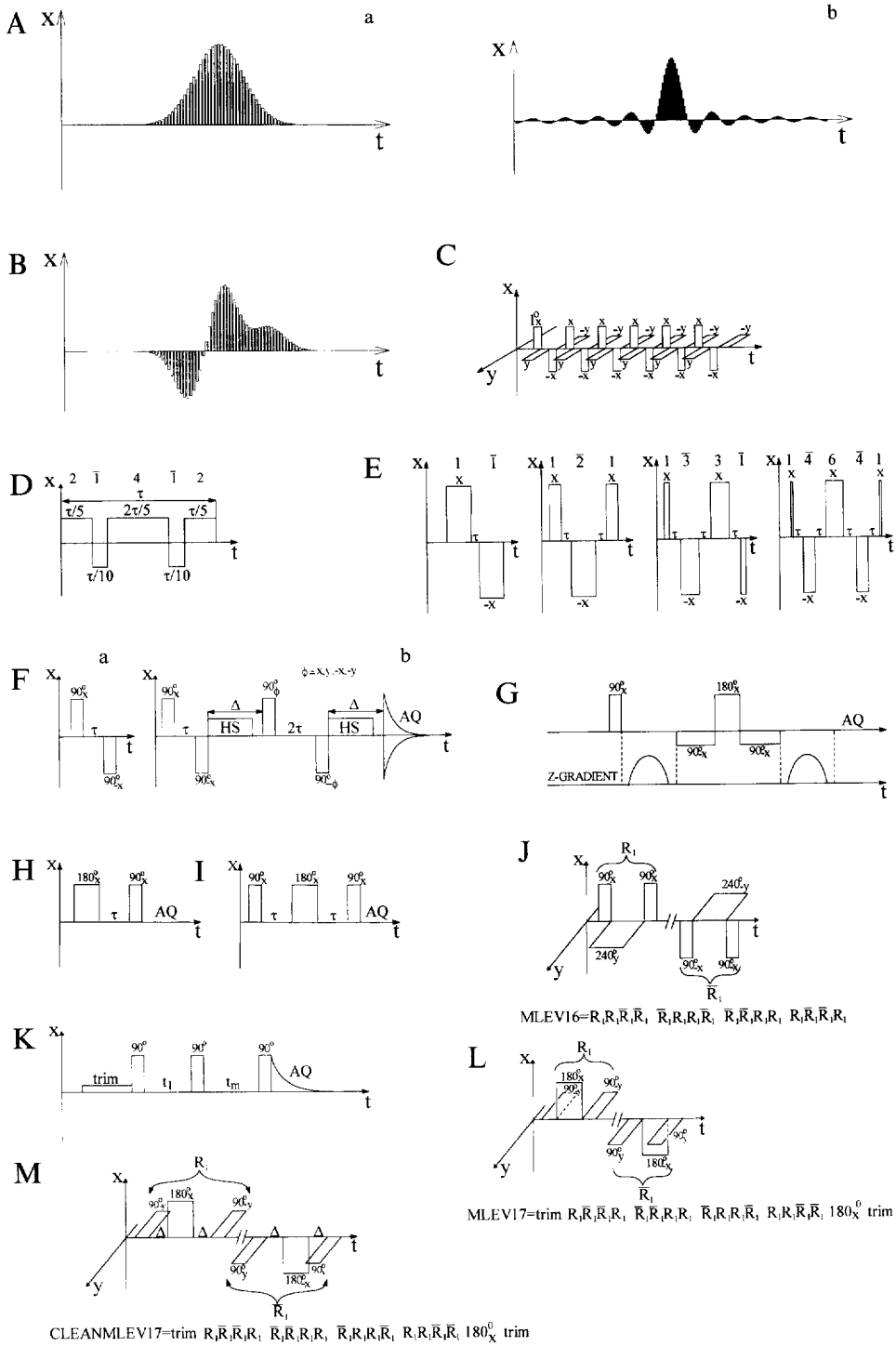

MLEV16=$R_1R_1\bar{R}_1\bar{R}_1$ $\bar{R}_1R_1R_1\bar{R}_1$ $\bar{R}_1\bar{R}_1R_1R_1$ $R_1\bar{R}_1\bar{R}_1R_1$

MLEV17=trim $R_1\bar{R}_1\bar{R}_1R_1$ $\bar{R}_1\bar{R}_1R_1R_1$ $\bar{R}_1R_1R_1\bar{R}_1$ $R_1R_1\bar{R}_1\bar{R}_1$ 180^0_x trim

CLEANMLEV17=trim $R_1\bar{R}_1\bar{R}_1R_1$ $\bar{R}_1\bar{R}_1R_1R_1$ $\bar{R}_1R_1R_1\bar{R}_1$ $R_1R_1\bar{R}_1\bar{R}_1$ 180^0_x trim

allows one to set the carrier frequency at any position with respect to the signal to be presaturated. Such a goal is obtained [6] by subdividing the long presaturation pulse having the low power required to saturate the signal, into a large number of short pulses of the same power with durations corresponding to $\frac{1}{4}$ of the reciprocal of the difference in frequency between the carrier and the signal of interest. The phase of the pulses is incremented by 90° each time, for instance with the scheme $x, y, -x, -y$ (Fig. 9.1(C)). In this way, after the first pulse the z magnetization of the signal is slightly tilted towards the xy plane and its xy projection has simultaneously precessed by 90°. Therefore, the effect of the second pulse is additive, producing a further tilt toward the xy plane, and so on (Fig. 9.2). Other signals with different carrier frequency end up being periodically out of phase with the pulse phase cycle, and the overall effect is zero. The order in which the phase of the pulses is incremented determines the sign of the offset. For instance, an offset of −2000 Hz is selected by using a time of $1/(4 \times 2000) = 0.125$ ms and the pulse phases $x, -y, -x, y$.

9.1.2. Selective non-excitation

It is possible to shape an excitation profile with weak pulses in such a way as to have zero excitation at a certain frequency. This was first due to Redfield [7]. The carrier must be placed in the region of the signals to be excited. The $2\bar{1}4\bar{1}2$ Redfield pulse sequence reported in Fig. 9.1(D) is a suitable example [7]. The total composite pulse duration must be set equal to the reciprocal of the offset of the signal to be non-excited. The carrier can also be located on the unwanted signal, and one of the many binomial pulse sequences (see Fig. 9.1(E)) can be used. Binomial pulses are made of strong rather than weak pulses, interleaved by delays [8,9]. The general concept of the effect of strong pulses can be illustrated by the simple "Jump and Return" (JR) sequence (Fig. 9.1(F)), constituted by a 90° pulse followed by a time τ followed by a −90° pulse [10]. If τ is sizably shorter than T_1, the magnetization of the signal at the carrier is first brought along the y axis and then back to the z axis. Signals whose offsets equal $\pm 1/2\tau$ move from the y axis to the $\pm x$ axis after the time τ; therefore, the second −90° pulse leaves them unaltered (see Fig. 9.3). The whole excitation profile is centered at frequencies $\pm 1/2\tau$ and has a width of $1/\tau$. Binomial sequences work similarly, but are constructed in such a way that the total pulse length sums up to a 90° pulse [8,9]. In our experience, the $1\bar{3}3\bar{1}$ sequence has given the best results. A general drawback of all these pulse sequences is that they produce strong baseline distortions. A pulse sequence analogous to the JR sequence which minimizes baseline distortions is the $1\bar{1}1\bar{1}$ sequence [11] (Fig. 9.1(F)).

Fig. 9.1. (A) Gaussian (a) and sinc (b) excitation profiles. (B) Composite (G3) Gaussian pulse. (C) Train of soft pulses modified after the DANTE sequence to achieve selective off-resonance excitation. (D) Redfield $2\bar{1}4\bar{1}2$ sequence. (E) Binomial $1\bar{1}$, $1\bar{2}1$, $1\bar{3}3\bar{1}$, $1\bar{4}6\bar{4}1$ sequences. (F) JR (a) and compensated JR (or $1\bar{1}1\bar{1}$) (b) sequences. (G) Watergate sequence. (H) Weft (Superweft) sequence. (I) Modeft sequence. (J) MLEV16 sequence. (K) NOESY sequence with trim pulse. (L) MLEV17 sequence with trim pulses. (M) Clean -TOCSY sequence.

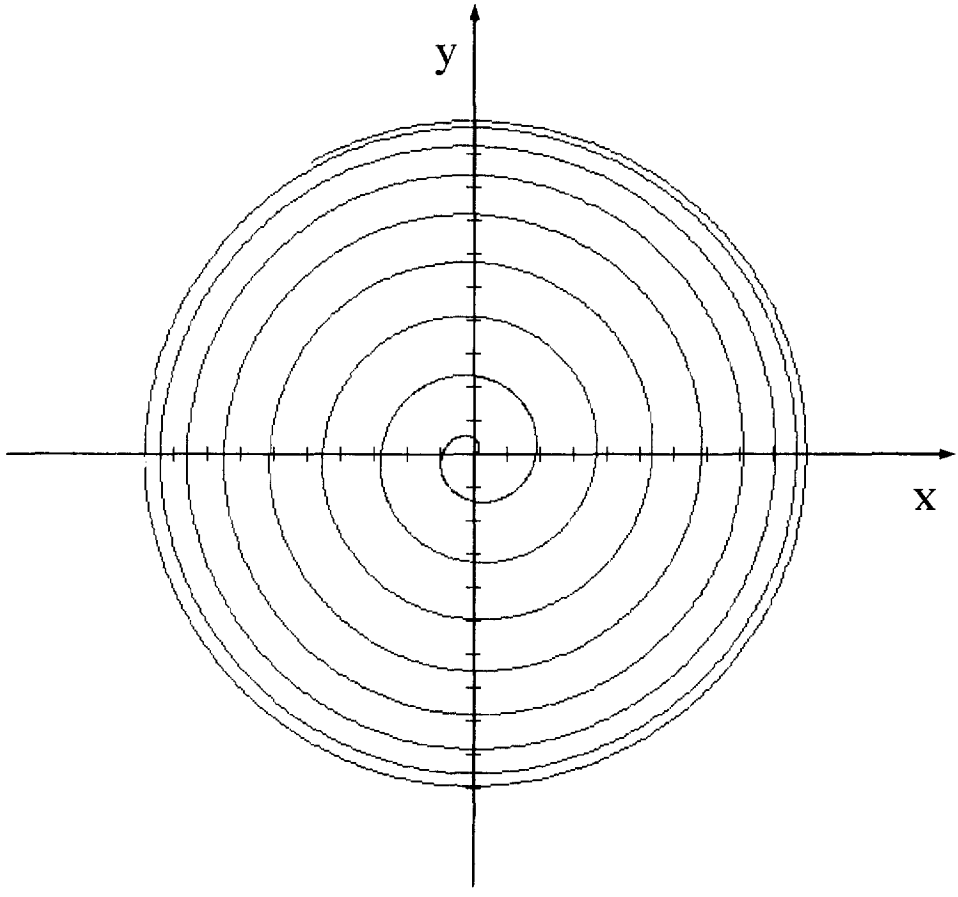

Fig. 9.2. Saturation effect of the modified DANTE sequence on a signal off-resonance with respect to the carrier frequency. The trajectory of the in-plane component of the magnetization is shown. The z magnetization is tilted by the first small angle pulse toward the x axis, and starts precessing toward the y axis. The duration of the pulse corresponds to the duration of a 90° precession, so that at the end of the first pulse the projection lies on the y axis. The phase of the following pulses is rotated in phase with the precession of the signal, in such a way as to "follow" the spin magnetization in its spiral movement toward the xy plane.

A very popular method for selective non-excitation employes field gradients along the z axis. After tilting the magnetization of all signals in the xy plane by a non-selective 90° pulse, a field gradient along z applied for a suitable time defocuses all the xy magnetization. If the time of application of the gradient is short enough that no appreciable T_2 relaxation, J modulation and molecular diffusion take place, the defocusing is reversible, and the xy magnetization can be fully recovered by the application of another gradient of opposite sign. Equivalently, the second gradient can be of the same sign of the first, provided that a 180° pulse is applied in between the two. In the so-called Watergate sequence [12], selective non-excitation is achieved

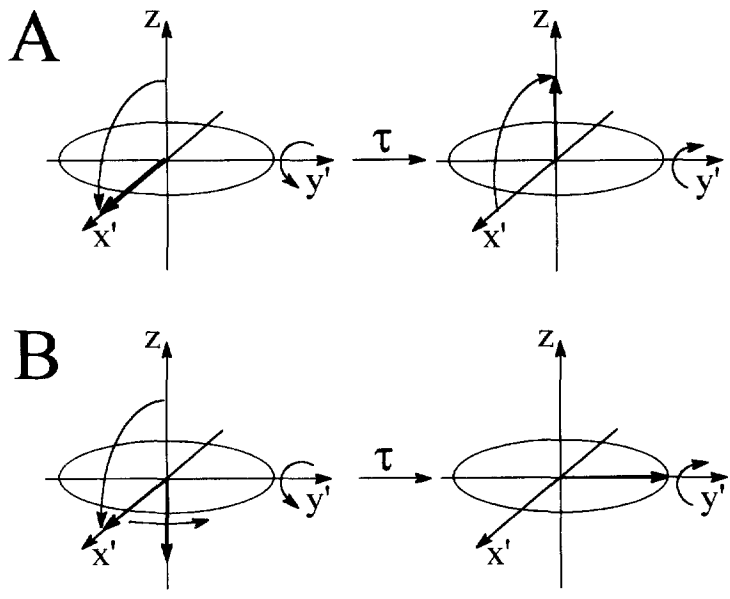

Fig. 9.3. Effect of the JR sequence on a signal on resonance (A) and off-resonance by $1/2\tau$ Hz (B).

by tailoring the 180° pulse in such a way that all frequencies but the unwanted frequency are irradiated. The simplest scheme employed a $90°_{-x}$(sel)$180°_{x}$(non-sel)$90°_{-x}$(sel) pulse sequence (Fig. 9.1(G)). The selectivity increases with the length of the 90° pulses.

The approach discussed in this section is preferable to any approach based on solvent suppression when solvent nuclei are in quasi-slow exchange with signals of interest. Saturation of the solvent nuclei transfers magnetization to the observable signals, decreasing their intensity, whereas non-excitation does not cause any interference.

9.1.3. *Selective suppression of signals with long T_1*

Whereas the two strategies of solvent suppression techniques described above do not show any particular advantage or disadvantage when applied to paramagnetic systems with respect to diamagnetic systems, the strategies based on differential relaxation properties have obvious intrinsic advantages in paramagnetic systems because of the larger spreading of nuclear relaxation times involved. The simplest approach to take advantage of the fast relaxation times of the signals of interest is that of acquiring the spectrum after a simple 90° pulse with a recycle time short with respect to the T_1 values of the signals to be suppressed, but long with respect to the T_1 values of the paramagnetic signals. Since the latter have also short T_2, short acquisition times are required. The consequence is that the slow relaxing signals are largely saturated, whereas the fast relaxing signals almost fully recover their initial

intensity after each cycle. Weft [13] and Superweft [14] pulse sequences (Fig. 9.1(H)) are based on the 180 τ 90 acquisition pulse sequence. When $\tau = T_1 \ln 2$ the signal with that T_1 has an intensity of zero. If the recycle time is longer than $5T_1$ (i.e. the system has fully recovered at each cycle) zero intensity of the signal of interest is maintained all over the experiment. This is the Weft pulse sequence [13]. During the time τ the fast relaxing signals have essentially recovered their magnetization and are detected. If the recycle time is chosen to be short with respect to the T_1 values of the signals to be suppressed, but long with respect to the T_1 values of the signals of interest, it has been shown that a τ value exists that after a few cycles, i.e. at steady state conditions, effectively zeroes the intensities of the signals with long T_1 [14]. An example of application of Superweft is provided in Fig. 9.4(A), where the spectrum of a protein containing a heme with low spin iron(III) in D_2O is reported [15]. This is obtained with a Superweft sequence with $\tau = 250$ ms and recycle time = 250 ms. The spectrum shows a number of well-resolved signals outside the diamagnetic region. When the signals of the axially-coordinated histidine are looked for, advantage is taken of the fact that they have T_1 values of the order of a few milliseconds, whereas the other hyperfine shifted signals have T_1 values of about 100 ms. Therefore, a Superweft with $\tau = 20$ ms and recycle time of 33 ms provides the spectrum of Fig. 9.4(B) where only the two non-exchangeable histidine ring protons are evident [15].

Weft or Superweft sequences are also widely used in 2D spectroscopies (see Section 9.4); in general, it is sufficient to place the 180°–τ part of the sequence in front of any 2D sequence to achieve the desired signal suppression.

The Modeft pulse sequence [16] drives the slow relaxing signals to equilibrium when the acquisition pulse is delivered. Modeft means modified driven equilibrium

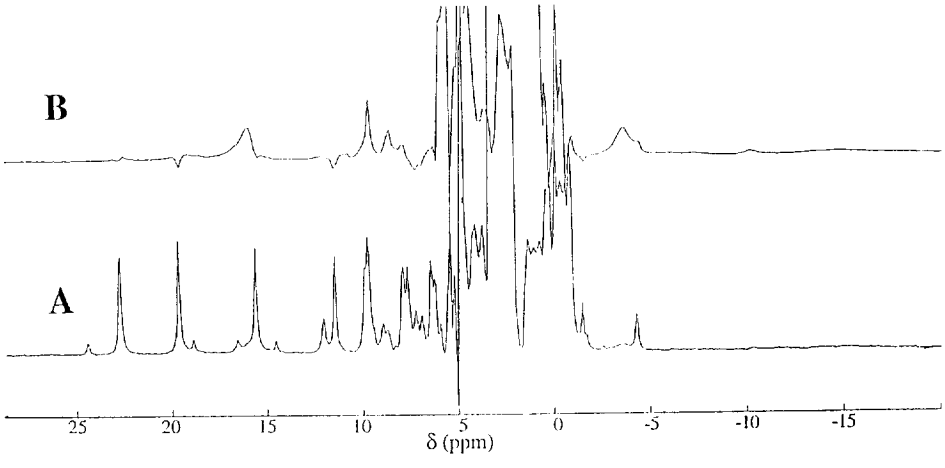

Fig. 9.4. 200 MHz ^{1}H NMR spectra in D_2O of the cyanide adduct of a cytochrome c mutant lacking the axial methionine (Ala80cyt c) recorded using the Superweft sequence with $\tau = 250$ ms and recycle time of 250 ms (A) and $\tau = 20$ ms and recycle time = 33 ms (B). In the latter spectrum the two signals of the axially-coordinated histidine are apparent at 16.1 and −3.4 ppm [15].

Fourier transform [17]. The pulse sequence is 90 τ 180 τ 90 acquisition (Fig. 9.1(I)). If τ is short with respect to T_1 the protons are driven to equilibrium. Signals with T_1 short with respect to τ recover after each pulse and the last 90° pulse acts as a normal excitation pulse. In Fig. 9.5 ^{1}H Modeft spectra of anion adducts of a cobalt(II) ($S = \frac{3}{2}$) protein of molecular weight 30 000 are shown [18]. The Modeft sequence is worse than the Superweft sequence in suppressing a single signal like the solvent signal, but performs comparably, and slightly better in some cases, when elimination of more than one slowly relaxing signal is needed. Typically, one might want to record a spectrum of a metalloprotein by the use of the superWEFT or the Modeft sequences when the few fast relaxing signals lying underneath the diamagnetic envelope of the many slowly relaxing signals are to be emphasized.

Other strategies to achieve this task are provided by the broadband (BB) saturation sequences (like MLEV16 (Fig. 9.1(J)) [19], WALTZ16 [20], GARP [21], DIPSI [22], etc.). The power of the BB saturation pulse can be adjusted in such a way as to effectively saturate the slowly relaxing signals and only marginally the fast relaxing ones. A 90° pulse immediately following the BB saturation sequence then gives a

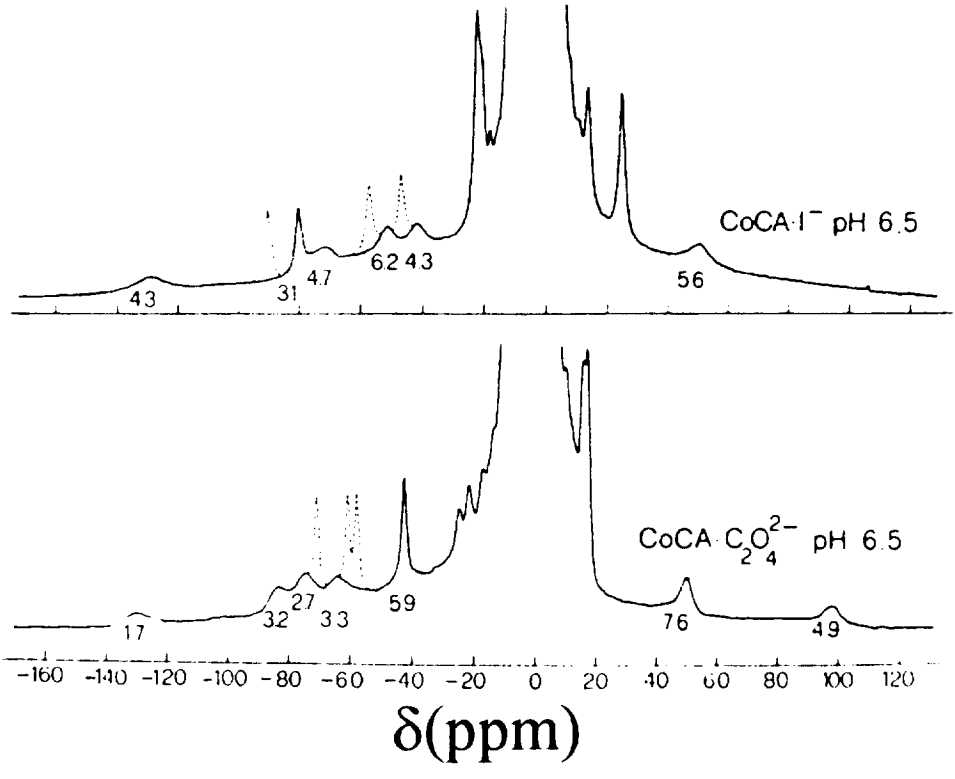

Fig. 9.5. 60 MHz ^{1}H NMR Modeft spectra of cobalt-substituted carbonic anhydrase (*MW* 30 000) adducts with iodide and oxalate. The T_1 values for some signals obtained with Eq. (9.1) (see later) are indicated. The dashed signals disappear in D_2O [18].

spectrum where the relative intensity of the fast relaxing signals is enhanced. Alternatively, the power of the BB saturation pulse can be high enough to saturate all signals. In this case, the following 90° detection pulse is applied after a time τ, adjusted in such a way that fast relaxing signals are appreciably recovered while slow relaxing signals are not.

While the Weft, Superweft and Modeft sequences are based on differences in T_1, BB saturation techniques are based on the difference in saturability of the signals, which in turn depends on $(T_1 T_2)^{1/2}$. Therefore, in cases where $T_2 \ll T_1$ for the paramagnetically affected signals (as can be the case in the presence of strong Curie relaxation), BB techniques may actually give better discrimination. Spin-lock techniques, based on differences in $T_{1\rho}$ ($\simeq T_2$), should perform best. However, applications of the latter are scarce, probably owing to the difficulty to efficiently irradiate a large spectral window.

9.1.4. *Choice of magnetic field*

As the major drawback in the observation of paramagnetic signals is ultimately the width of the lines, it is worth recalling again the various mechanisms causing line broadening. These mechanisms have been illustrated in Sections 3.4–3.6, and their relative importance has been discussed in Section 3.8. The relevant equations describing the three contributions to R_{2M} are Eqs. (3.14) (dipolar), (3.24) (contact) and (3.27) (Curie relaxation). The first two contributions to line broadening decrease with magnetic field (Figs. 3.10 and 3.12), while the third increases with magnetic field (Fig. 3.13). This observation suggests that the experimentalist may be able to use the magnetic field as a parameter to optimize signal detection. Developing this attitude is peculiar to paramagnetic NMR, as in general the field dependence of diamagnetic line broadening mechanisms is not pronounced enough to make the choice of the field critical. It is obvious that, in the absence of adverse effects, the higher the field, the better. In fact, if the linewidth (in hertz) is field-independent, the resolution increases linearly with the field: in other words, the linewidth in parts per million *decreases* with increasing field. However, Curie relaxation increases with the square of magnetic field. Therefore, when Curie relaxation is dominant, an increase in field will actually cause a decrease in resolution. In practice, Curie relaxation is dominant when its correlation time τ_r is much larger than τ_s, as in this case the latter is the dominant correlation time for dipolar and contact mechanisms. Furthermore, the importance of Curie relaxation increases with the electron spin quantum number S (or J for lanthanides), because dipolar and contact relaxation mechanisms depend on $S(S+1)$ (or $J(J+1)$), whereas Curie relaxation depends on the square of these quantities. Fig. 9.6 illustrates the field dependence of the linewidth (in parts per million) for a middle-sized macromolecular system ($\tau_r = 10^{-8}$ s) containing a fast relaxing paramagnetic metal ion ($\tau_s = 10^{-12}$ s) with S (or J) equal to $\frac{1}{2}$, $\frac{3}{2}$, $\frac{5}{2}$ and $\frac{7}{2}$. It appears that the optimal magnetic field decreases from about 400 MHz to 200 MHz, 120 MHz and 90 MHz. Note that these conditions are relatively common, and far from being extreme. In fact, τ_r values may be easily longer than 10^{-8} s (a τ_r of 10^{-8} s corresponds to a 30 000 MW protein); τ_s values may be shorter,

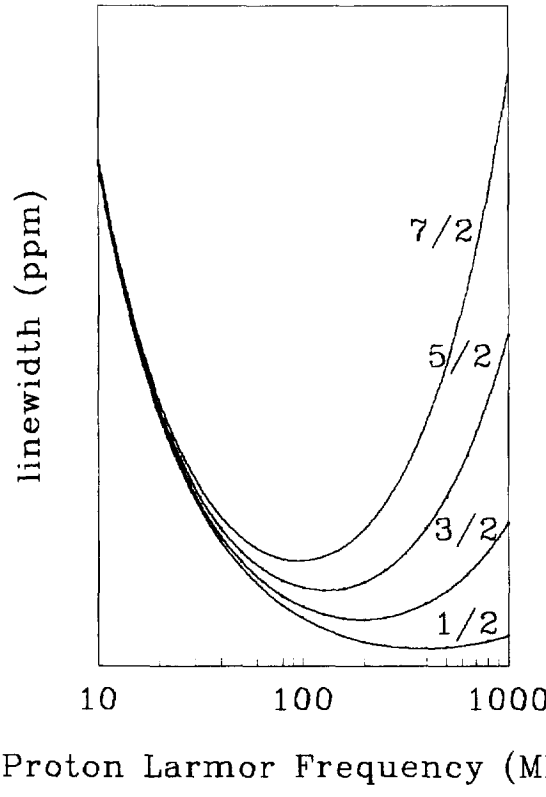

Fig. 9.6. Calculated field dependence of the linewidth (ppm) for a proton interacting with a paramagnetic metal ion in a macromolecule with $\tau_r = 10^{-8}$ s, $\tau_s = 10^{-12}$ s, and $S = \frac{1}{2}, \frac{3}{2}, \frac{5}{2}$ (or $J = \frac{7}{2}$ for a lanthanide).

and J values may be larger (for example in lanthanides, where τ_s values close to 10^{-13} s have been reported and J values can be as large as 8).

9.2. Measurements of T_1 and T_2

As far as T_1 is concerned, we should remember that longitudinal relaxation can be multiexponential. Therefore, different information can be obtained, depending on whether a given signal is selectively excited or it is excited together with other signals. We usually refer to T_1 as an experimental T_1 value obtained by assuming that the magnetization recovery is exponential. This is very often a better approximation in paramagnetic systems than in diamagnetic ones, because the unpaired electron acts as a sink for nuclear spin energy, thereby making the whole magnetization recovery closer to a single exponential (Sections 1.7.4 and 6.2.2). When a single signal is

excited, we refer to selective T_1, which is thus distinguishable from a non-selective T_1 obtained when more signals are simultaneously excited.

Non-selective T_1 can be measured with the usual inversion recovery 180 τ 90 pulse sequences [23]. It should be noted that, if the frequency range covered is large, the 180 or even the 90 pulse may not be the same all over the spectral region of interest. It may then be convenient to select ranges of excitation. Sometimes it may be convenient to measure T_1 with the Modeft pulse sequence 90 τ 180 τ 90: by making τ shorter and shorter we eventually have zero intensity also of the fast relaxing signals. The signal intensity as a function of τ is given by [16]

$$M_z(\tau) = M_z(\infty)[1 - 2\exp(-R_1\tau) + (1 - a)\exp(-2R_1\tau)] \tag{9.1}$$

where $R_1 = T_1^{-1}$ and a is a parameter that compensates for misadjustments of the first 90° pulse.

Selective T_1 values are generally measured with the 180 τ 90 pulse sequence using a soft 180° pulse. When the nuclear relaxation times are short, it may become impossible to invert the magnetization and at the same time maintain the required selectivity with the soft pulse. When such difficulties arise, a good compromise is to use a soft pulse that can at least saturate the signal. Then, the sequence becomes equivalent to a 90 τ 90 pulse sequence.

Fast relaxing nuclei are characterized by a sizable linewidth. The measurement of the linewidth represents the easiest and most straightforward way of measuring T_2^{-1} from the relationship

$$T_2^{-1} = \pi\Delta\nu \tag{9.2}$$

where $\Delta\nu$ is the linewidth at half peak height. Such procedure is absolutely adequate in paramagnetic systems when the lines are relatively large, since the relative contribution of field inhomogeneity is in any case small. Of course, when the linewidth becomes narrow, as in a diamagnetic system, the usual Carr–Purcell–Meiboom–Gill (CPMG) technique [24] should be used.

In the case of T_1 measurements we have mentioned that cross relaxation provides multiexponential magnetization recovery (Sections 1.7.4 and 6.2.2). A far less known analogy may occur in the linewidths, as already discussed (Section 7.8) when two protons are dipole–dipole coupled and cross correlation occurs between Curie relaxation and proton–proton dipolar relaxation. In this case, we are in the presence of two overlapping signal components with different linewidths, i.e. of biexponentiality in T_2 [25]. Pulse sequences are available to remove the effects of cross correlation [26]. Such effects are common in paramagnetic metalloproteins where Curie relaxation is usually relevant (in principle, such cross correlation effects can be operative also in the case of T_1, although only to the extent that Curie relaxation on T_1 is effective).

9.3. Measurements of NOE

The nuclear Overhauser effect was predicted in 1953 [27], experimentally demonstrated in 1955 [28], and widely used since then to obtain structural and conformational information in diamagnetic small molecules. As it appears from Section 6.2,

NOEs are small and positive in small molecules. Cross relaxation is small and spin diffusion effects are also small. When the rotational correlation time increases, the sign of the NOE becomes negative, the absolute value increases, and cross relaxation effects become larger. As a result of the latter effects, the so-called spin diffusion takes place, which makes less straightforward the interpretation of the relationship between NOE and internuclear distances. In diamagnetic macromolecules, nuclear Overhauser effects are almost exclusively measured through 2D or 3D experiments, and distance information often extracted with the help of proper algorithms. In small molecules, 1D NOE is still used to obtain accurate selected internuclear distances when the signals are well separated.

The 1D NOE technique has had a strong revival when applied to paramagnetic molecules. Here the signals to be irradiated can be well separated (hyperfine shifted), nuclear relaxation is more affected by the coupling with the unpaired electrons than by the coupling with other protons and, if the molecule is large, large effects can be measured without the drawback of having all the signals in a narrow spectral region. If one is at the extreme limit of detectability of dipolar connectivities (as is often the case in fast relaxing and relatively diluted samples), 1D NOE is the most suitable technique, as discussed in Chapter 6.

As discussed in Sections 9.1.1 and 9.1.3, it is difficult to saturate in a selective way a fast relaxing signal. Selectivity here is an absolute requirement because the wings of the excitation profile of a soft pulse may well partially saturate other signals, with the consequence of appearance of artifacts which vary from case to case but may lead to gross misinterpretations. The use of suitably shaped pulses designed to be more selective than a rectangular pulse is advisable. Even with a perfectly selective irradiation, other signals can be partly saturated because their tails may extend down to where the irradiation is applied. To further remove the residual effects of non-perfect selectivity and of tail excitation, the most common procedure is that of alternating experiments with the saturation pulse applied on-resonance and off-resonance, and subtracting the latter from the former. Even so, off-resonance effects on signals very close to the irradiated one cannot be readily discriminated from true NOEs that in macromolecules are negative. Fig. 9.7(A) provides a clear example [29]. Upon irradiation of signal *g*, signal *f* gives NOE while signal *d* is affected by off-resonance effects. This could be demonstrated by performing an irradiation "profile" (Fig. 9.7(B)): the effect of *f* is maximal when the irradiation frequency is on *g*, whereas the effect on *d* steadily increases with increasing irradiation frequency [29].

In our experience, the best experimental scheme is to choose two off-resonance positions symmetrical with respect to the irradiated signal and typically offset by one to two times the linewidth of the irradiated signal (Fig. 9.8).

It often happens that there is at least one signal too close to the signal to be irradiated to allow for the setting of the two off-resonance frequencies in the optimal position. In fact, if another signal is close to one of the two off-resonance frequencies, in the difference spectrum this signal appears as strongly positive. If this signal gives NOEs with the same signal(s) which experience NOE from the irradiated signal, the two NOEs are opposite in sign and the unwanted one may reduce or cancel the one which is looked for. A general strategy to eliminate this effect is to place the off-

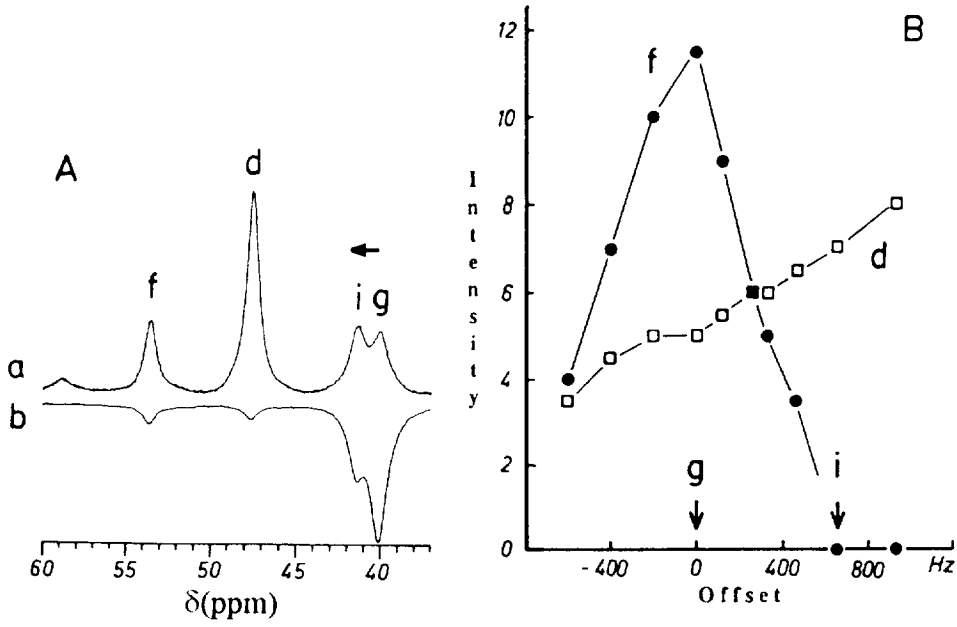

Fig. 9.7. 1D NOE difference experiments on met-aquo myoglobin. (A) Reference spectrum *a* and difference spectrum *b* observed upon saturation of peak *g*. (B) Intensity of negative *f* and *d* signals in *b* as a function of the irradiation frequency. Signal *f* is maximal when the irradiation frequency is on *g*, signal *d* shows a steady increase with increasing frequency [29].

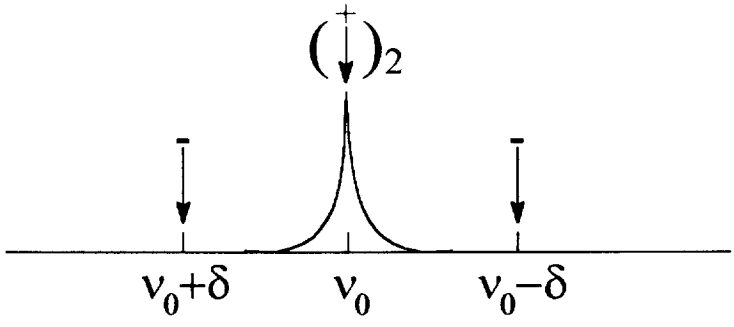

Fig. 9.8. Irradiation scheme used in NOE experiments to minimize off-resonance effects. The r.f. is alternately placed at ν_0, $\nu_0+\delta$, ν_0, $\nu_0-\delta$. The spectra obtained upon irradiation at $\nu_0 \pm \delta$ are subtracted from those obtained upon irradiation at ν_0.

resonance offset beyond the unwanted signal. If the offset is far enough, the latter signal is now negative for macromolecules, since the off resonance from the central irradiation position is dominant. It is easy to show that an off-resonance position always exists for which the intensity of the unwanted signal is rigorously zero. The other offset is, of course, always symmetrical with respect to the irradiated signal. The optimal position can be determined empirically with a small number of scans before starting the real experiment. In Fig. 9.9, the spectrum of the oxidized high

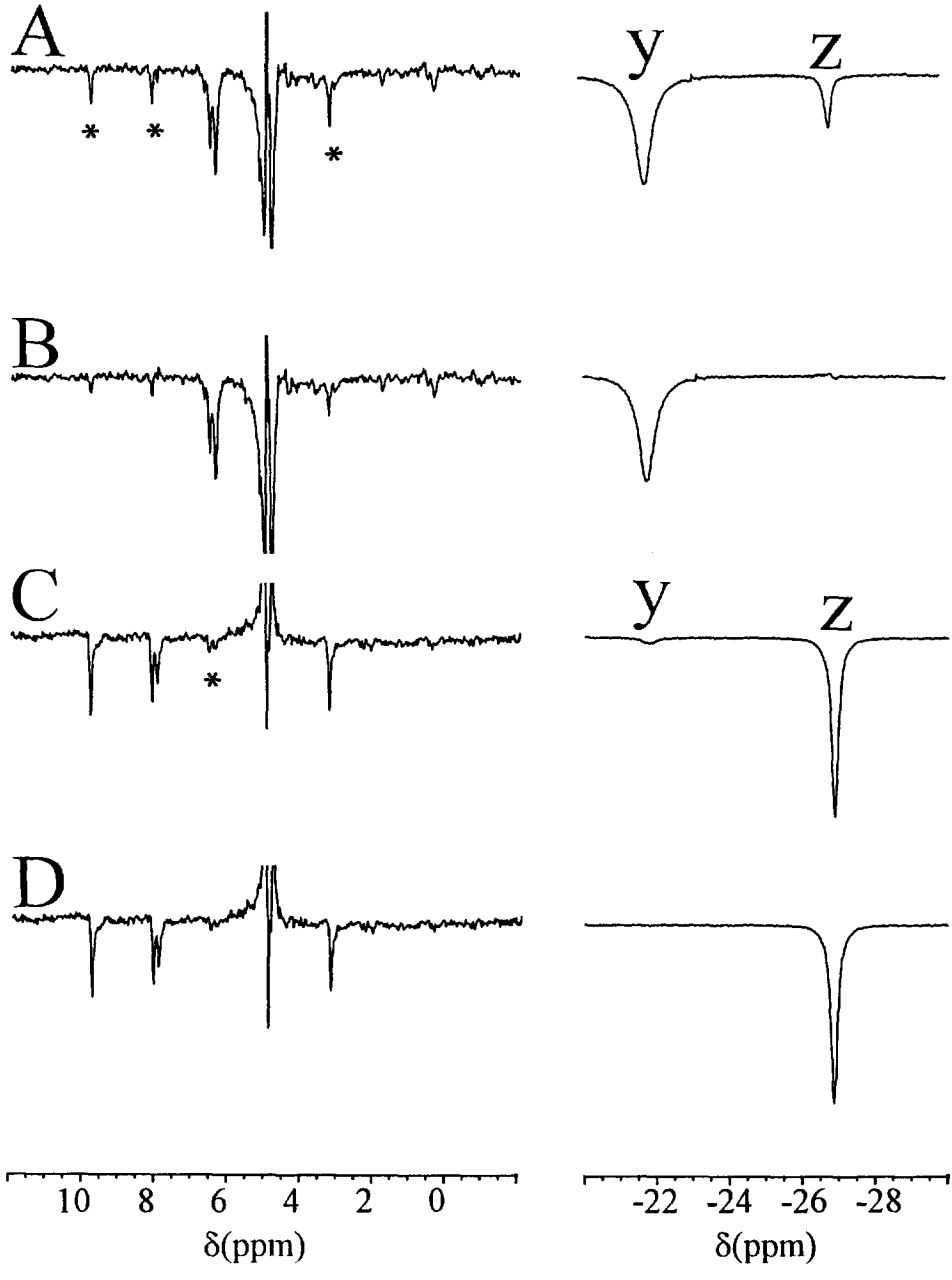

Fig. 9.9. 600 MHz 1D NOE difference spectra of the oxidized form of the high potential Fe_4S_4 protein from *E. halophila* iso I [30]. Spectra (A) and (C) are obtained by irradiating each of the two geminal β-CH_2 protons (*y* and *z*) of the cluster-ligated Cys-39. Spectrum (B) is obtained by subtracting from spectrum (A) spectrum (C) multiplied by a factor such that signal *z* is canceled; spectrum (D) is obtained by subtracting from spectrum (C) spectrum (A) multiplied by a factor such that signal *y* is canceled. Note the reduction of intensity of the signals marked with asterisks.

potential iron–sulfur protein from *E. halophila* iso I is reported [30], together with the NOE difference spectra obtained upon saturation of signals *y* and *z*, using the above irradiation scheme. Signals *y* and *z* happen to be geminal β-CH_2 protons of the same cysteine residue and to have rather long T_1 values. Therefore, despite the optimization of the off-resonance frequencies, a sizable real NOE is present from one signal to another in both cases. To further eliminate the secondary NOEs from the geminal signal, double difference NOE spectra were obtained by subtracting from one NOE difference spectrum the other one, appropriately scaled.

Approaches of this kind are also particularly important when the NOE to be observed is on a signal close to the irradiated one. In the case of the two β-CH_2 protons of an Asp residue bound to a high spin cobalt(II) in the protein superoxide dismutase, the two signals *D* and *E* are very broad (Fig. 9.10(A)). The NOE between the two signals has been observed by irradiating signal *D* and by recording the difference spectrum with one off-resonance position symmetrical with respect to the position of signal *E* [31]. In principle, in this way any intensity detected at the *E* position is due to a real NOE. In practice, a strong distortion of the baseline at the *E* position is present because of the tails of signal *C*, experiencing off-resonance from *D*. Another experiment is performed by irradiating this third signal with the off-resonance position still symmetrical with respect to *E*, and by further subtracting the two NOE difference spectra one from the other. The double difference NOE spectrum is shown in Fig. 9.10(B).

It is often necessary to obtain a profile of NOE intensities vs. the irradiation time, called NOE buildup. A series of truncated NOEs are thus needed (Section 6.3). The only caveat with respect to buildup experiments in a diamagnetic case is that there is a lower limit in the irradiation time because even a truncated NOE needs saturation of the irradiated signals. Since "instantaneous" saturations are not possible, but short saturation times are needed to measure the first points of the buildup, there is the risk that at the beginning of the buildup the irradiated signal is not 100% saturated [29]. In practice, buildup measurements are feasible when the irradiated signal relaxes faster than the responding signals, but hardly when the reverse is true. Even in the most favorable case, the intensities of the very first points may not be accurate; as a consequence, it is always a risk to use buildup experiments to discriminate between primary and secondary NOEs. However, in paramagnetic systems, secondary NOEs are usually small and, in general, recognizable from other indirect evidence (see Chapter 6).

As far as the transient NOE is concerned, the problem of the selective 180° pulse has already been addressed. The non-optimal selectivity leads to dramatic artifacts [32]. Therefore, transient NOE is not the technique of choice in paramagnetic systems [33].

9.4. 2D spectra

9.4.1. NOESY

When setting a NOESY experiment on a paramagnetic molecule the mixing time t_m should be of the order of the T_1 of the signals between which cross peaks are

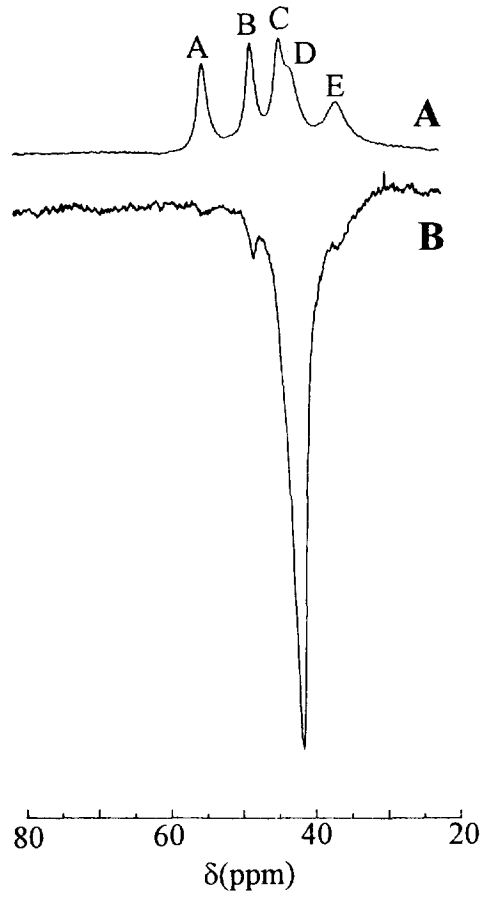

Fig. 9.10. (A) 200 MHz ^{1}H NMR spectrum of copper-depleted, cobalt-substituted Cu,Zn superoxide dismutase; (B) difference between the difference NOE spectra obtained by irradiating signals *D* and *C* respectively. The spectra demonstrate that the NOE on *E* arises from *D* and not from *C*. The off-resonance position was placed symmetrical with respect to *E* in both cases [31].

looked for. When the T_1 values are very different, and this is common in paramagnetic molecules, especially if there are protons close to the paramagnetic center and protons far from it, the best mixing time should be calculated case by case from Eq. (7.1). For the reader's convenience, Table 7.1 is provided, with the relative T_1 values spanning two orders of magnitude. Note that, when the T_1 values are very different, the best mixing time, which is always intermediate between the two T_1 values, can be as large as five times the shorter T_1 (Section 7.3).

A comment is due to the comparison of the intensity of a steady state NOE with that of a transient NOE in the case of signals with different T_1 values. This is because the intensity of a NOESY cross peak is related to the intensity of a transient NOE (Sections 6.4 and 7.3) and because in paramagnetic systems we may be at the lower

limit of cross peak detectability. Therefore, a steady state NOE obtained by saturating the fast relaxing signal is always advisable to extend the detectability of its dipolar connectivities as much as possible. Table 9.1 shows the advantage of steady state vs. transient NOE for a range of ratios of T_1 values. It appears that steady state NOE is always superior to transient NOE, except when the T_1 of the irradiated signal is longer than that of the responding signal by more than a factor of two. In paramagnetic metalloproteins, the faster relaxing signals are often outside the diamagnetic envelope and are separated one from the other, so that they can be irradiated quite easily. The slower relaxing signals are often in the diamagnetic envelope. It is therefore a good practice to measure the steady state NOE by irradiating each of them prior to performing 2D experiments.

In summary, when performing a NOESY spectrum of a paramagnetic molecule containing both fast and slow relaxing nuclei, it is convenient: (1) to record a NOESY spectrum with a mixing time which matches the short relaxation times in order to detect connectivities between fast relaxing signals; (2) to record a NOESY spectrum

Table 9.1
Comparison between steady state (SS) and maximal transient (TR) NOE intensities (%) for various T_1 (ρ^{-1}) values (ms) of the two spins I and J, calculated using Eqs. (6.10) and (6.19) (the negative signs are omitted). The calculations are performed for a $\sigma_{I(J)}$ value of $-1\ s^{-1}$. Steady state NOE is always superior to transient NOE, except when T_1^I of the irradiated signal is more than twice the T_1^J of the responding signal (upper right part of the table)

T_1^I		T_1^J							
		128	64	32	16	8	4	2	1
128	SS	12.80	6.40	3.20	1.60	0.80	0.40	0.20	0.10
	TR	9.44	6.40	4.03	2.38	1.33	0.72	0.37	0.19
64	SS	12.80	6.40	3.20	1.60	0.80	0.40	0.20	0.10
	TR	6.41	4.71	3.20	2.02	1.19	0.67	0.36	0.19
32	SS	12.80	6.40	3.20	1.60	0.80	0.40	0.20	0.10
	TR	4.03	3.20	2.35	1.60	1.01	0.59	0.33	0.18
16	SS	12.80	6.40	3.20	1.60	0.80	0.40	0.20	0.10
	TR	2.38	2.02	1.60	1.18	0.80	0.50	0.30	0.17
8	SS	12.80	6.40	3.20	1.60	0.80	0.40	0.20	0.10
	TR	1.33	1.19	1.01	0.80	0.59	0.40	0.25	0.15
4	SS	12.80	6.40	3.20	1.60	0.80	0.40	0.20	0.10
	TR	0.72	0.67	0.59	0.50	0.40	0.29	0.20	0.13
2	SS	12.80	6.40	3.20	1.60	0.80	0.40	0.20	0.10
	TR	0.37	0.36	0.33	0.30	0.25	0.20	0.15	0.10
1	SS	12.80	6.40	3.20	1.60	0.80	0.40	0.20	0.10
	TR	0.19	0.19	0.18	0.17	0.15	0.13	0.10	0.07

with a mixing time which matches the relaxation times of the slow relaxing nuclei in order to detect connectivities between slow relaxing signals; (3) to record a NOESY with a mixing time taken from Table 7.1 depending on the T_1 of the fast and slow relaxing nuclei in order to detect connectivities between fast and slow relaxing signals; (4) to measure the steady state NOEs by saturating the fast relaxing signals in order to be sure to detect connectivities with slow relaxing nuclei as much as possible.

A further parameter in measuring NOESY spectra is the recycle time. In small molecules it should be ideally five times the longest T_1 of the signals for which connectivities are looked for. The $5T_1$ is needed to let the nuclei of interest recover their magnetization. In macromolecules such time is better set approximately equal to the longest T_1 among the signals of interest: the loss in cross peak intensity is overcome by the gain in number of cycles within the same experimental time. When recording a NOESY spectrum with a short recycle time the transverse magnetization of the slow relaxing signals has no time to disappear before the next scan; this gives rise to various artifacts in the 2D spectrum. For this reason, a CW pulse of the duration of some milliseconds, called trim pulse, can be used to destroy transverse coherence before the following experiment. A convenient pulse sequence is shown in Fig. 9.1(K). The intensity of the pulse should be set according to the spectral region over which the trim is needed. Typically, trim pulses of the order of 1 ms are used for paramagnetic systems.

In a NOE–NOESY experiment (Section 7.9) the connectivities between a fast relaxing signal and a set of slow relaxing signals are obtained simultaneously with those within the above set of slow relaxing signals. Therefore the NOESY parameters should be set according to the slow relaxing signals.

9.4.2. COSY and spin-lock experiments

A typical COSY sequence is 90 τ 90 acquisition. If two signals A and B are coupled by scalar interactions, a cross peak is expected. The shape of the cross peak depends on several factors. The first one regards whether the signal linewidths are smaller or larger with respect to J. In the former case, the cross peak consists of four components arranged on a square and separated by J. The four components have antiphase structure, i.e. in a phase-sensitive experiment phased in absorption mode there are two positive and two negative peaks. The routine phase-sensitive experiment introduces sensitivity to the phase, which allows the operator to choose absorption or dispersion mode for the cross peaks. There is no advantage in choosing the dispersion mode because a line in dispersion mode is broader than in absorption mode. In magnitude mode the phase is lost and all four peaks are positive.

In the case in which T_2^{-1} is larger than J, one would think that the antiphase character of the cross peaks in the TPPI mode cancels partially or totally the cross peaks. Indeed, much of the intensity of the signal is lost. The loss can, however, be reduced if the cross peaks are phased in dispersion mode [34] or if the experiments are performed in magnitude mode [26] (Section 7.5). The occurrence of coherence

transfer phenomena may give rise to COSY cross peaks even in the absence of scalar coupling (Section 7.8) [25]. As long as this is kept in mind, COSY cross peaks between very broad lines can be looked for, and interpreted as dipolar correlation cross peaks.

TOCSY spectra are critical to perform on paramagnetic systems when the required spectral window is large, because of the need to irradiate the spectral window efficiently with each component of a long train of many pulses (like for instance the MLEV17 sequence [35], Fig. 9.1(L)). Overheating of the sample can occur, and in extreme cases the probe coil may not stand the pulse power for the required time. Other spin lock sequences constructed from WALTZ [20] or DIPSY [22]-type sequences may allow some reduction of the power needed, the spectral window being the same.

Another improvement with respect to these problems is represented by the so-called Clean-TOCSY experiment [36]. Clean-TOCSY was originally devised to avoid the build up of ROE during a TOCSY experiment. In small molecules ROE cross peaks in a TOCSY spectrum may be mistaken for scalar TOCSY cross peaks, while in large molecules, where ROESY and TOCSY have opposite signs, the presence of ROESY may accidentally cancel TOCSY cross peaks. In Clean-TOCSY, short delays are interleaved between the pulses of the MLEV17 sequence (Fig. 9.1(M)) in such a way that the ROE effect is lost. This has also the side-effect that, for the same overall spin lock time t_m, less energy (power × time) is delivered to the sample. Therefore, the length of each pulse can be, for instance, halved, and its power doubled without delivering to the sample more energy than in the original TOCSY experiment. In principle, even full high power pulses can be used, provided that enough delay is interleaved between them.

9.5. Suggestions for spectral assignment

At the end of this book it may be useful to summarize a possible strategy for spectral assignments. Some hints are so simple that they have never been mentioned previously, whereas other hints are implicit in the various parts of the book.

When analyzing a proton NMR spectrum one should look at the intensities of the signals in a spectrum acquired with recycle time much longer than the T_1 values of the signals. This helps in deciding whether the signal belongs, for instance, to a methyl or to a set of magnetically equivalent nuclei. Another obvious criterion is to compare the spectra where a proton in a given position is substituted by another nucleus.

The first criterion really related to the content of this book is the analysis of T_1 and T_2. As the dominant contribution to nuclear relaxation is dipolar in nature, T_1^{-1} and linewidths will decrease as we move farther from the paramagnetic center. Even the contact contribution to relaxation often decreases with the number of chemical bonds from the paramagnetic center. A caveat, however, should be given. Spin density transfer causes ligand-centered relaxation. Significant spin density on a π orbital of an sp^2 carbon may relax an attached proton more than the paramagnetic

center itself, owing to the different distances and to the sixth power dependence on distance.

With relaxation data at hand, and with some experience, a tentative assignment can be proposed. This is how NMR spectroscopists of paramagnetic molecules operated from the 1960s to the 1980s. The first order J splitting is only rarely observed in paramagnetic molecules, and therefore is not a useful tool for the assignment.

At this point NOE and NOESY experiments are needed. In this way we learn which proton is close to which other proton, and the picture becomes sharper. Sometimes, when the correlation times governing cross relaxation are unfavorable, ROE or ROESY experiments can be a valid alternative. Both NOE and ROE types of experiment also provide information on the presence of chemical equilibria when the interconversion rate is of the order of T_1. It is also clear that NOE and ROE types of experiment may not always provide a unique picture, because they ignore chemical bonds. COSY and TOCSY experiments provide the information on which proton is chemically bound to which other proton. The assignment at this point should not be tentative any more, but based on a so-called modern NMR approach.

The last consideration regards the pattern of spin densities, which should match with expectations based on the possible delocalization mechanisms illustrated in Chapter 2.

If high sample concentrations can be reached, ^{1}H–^{13}C Hetcor experiments can be performed and further information can be obtained to study spin density patterns. If then the sample can be enriched with ^{13}C or ^{15}N, experiments are available to determine J couplings involving ^{1}H, ^{13}C, ^{15}N, ^{31}P, etc. The J values contain structural information, and therefore can be used for assignment. Owing to the small γ values, the potentiality of heteronuclei in paramagnetic molecules has still to be further investigated.

References

[1] C. Bauer, R. Freeman, T. Frenkiel, J. Keeler and A.J. Shaka, J. Magn. Reson., 58 (1984) 442.
[2] A.J. Temps, Jr. and C.F. Brewer, J. Magn. Reson., 56 (1984) 355.
[3] W.S. Warren, J. Chem. Phys., 81 (1984) 5437.
[4] L. Emsley and G. Bodenhausen, Chem. Phys. Lett., 165 (1990) 469.
[5] G.A. Morris and R. Freeman, J. Magn. Reson., 29 (1978) 433.
[6] L.E. Kay, D. Marion and A. Bax, J. Magn. Reson., 84 (1989) 72.
[7] A.G. Redfield, S.D. Kunz and E.K. Ralph, J. Magn. Reson., 19 (1975) 114.
[8] D.L. Turner, J. Magn. Reson., 54 (1983) 146.
[9] P.J. Hore, J. Magn. Reson., 55 (1983) 283.
[10] P. Plateau and M. Gueron, J. Am. Chem. Soc., 104 (1982) 7310.
[11] V. Sklenar, and A. Bax, J. Magn. Reson., 74 (1987) 469.
[12] M. Piotto, V. Saudek and V. Sklenar, J. Biomol. NMR, 2 (1992) 661.
[13] S.L. Patt and B.D. Sykes, J. Chem. Phys., 56 (1972) 3182.
[14] T. Inubushi and E.D. Becker, J. Magn. Reson., 51 (1983) 128.
[15] K.L. Bren, H.B. Gray, L. Banci, I. Bertini and P. Turano, J. Am. Chem. Soc., 117 (1995) 8067.
[16] J. Hochmann and H. Kellerhals, J. Magn. Reson., 38 (1980) 23.

[17] E.D. Becker, J.A. Ferretti and T.C. Farrar, J. Am. Chem. Soc., 91 (1969) 7784.
[18] I. Bertini, G. Canti, C. Luchinat and F. Mani, J. Am. Chem. Soc., 103 (1981) 7784.
[19] M.H. Levitt, R. Freeman and T. Frenkiel, J. Magn. Reson., 47 (1982) 328.
[20] A.J. Shaka, J. Keeler and R. Freeman, J. Magn. Reson., 53 (1983) 313.
[21] A.J. Shaka, P.B. Barker and R. Freeman, J. Magn. Reson., 64 (1985) 547.
[22] A.J. Shaka, C.J. Lee and A. Pines, J. Magn. Reson., 77 (1988) 274.
[23] R.L. Vold, J.S. Waugh, M.P. Klein and D.E. Phelps, J. Chem. Phys., 48 (1968) 3831.
[24] S. Meiboom and D. Gill, Rev. Sci. Instrum., 29 (1958) 688.
[25] I. Bertini, C. Luchinat and D. Tarchi, Chem. Phys. Lett., 203 (1993) 445.
[26] I. Bertini, C. Luchinat, M. Piccioli and D. Tarchi, Concepts Magn. Reson., 6 (1994) 307.
[27] A.W. Overhauser, Phys. Rev., 89 (1953) 689.
[28] I. Solomon, Phys. Rev., 99 (1955) 559.
[29] J.T.J. Lecomte, S.W. Unger and G.N. La Mar, J. Magn. Reson., 94 (1991) 112.
[30] L. Banci, I. Bertini, F. Capozzi, P. Carloni, S. Ciurli, C. Luchinat and M. Piccioli, J. Am. Chem. Soc., 115 (1993) 3431.
[31] L. Banci, I. Bertini, C. Luchinat and M.S. Viezzoli, Inorg. Chem., 29 (1990) 1438.
[32] M. Paci, A. Desideri, M. Sette, M. Falconi and G. Rotilio, FEBS Lett., 261 (1990) 231.
[33] L. Banci, I. Bertini, C. Luchinat and M. Piccioli, FEBS Lett., 272 (1990) 175.
[34] A.V. Xavier, D.L. Turner and H. Santos, Methods Enzymol., 227 (1993) 1.
[35] A. Bax and D.G. Davis, J. Magn. Reson., 65 (1985) 355.
[36] C. Griesinger, G. Otting, K. Wüthrich and R.R. Ernst, J. Am. Chem. Soc., 110 (1988) 7870.